

Testing an unifying view of Gamma Ray Burst afterglows

M. Nardini*, G. Ghisellini, G. Ghirlanda[†] and A. Celotti**

*SISSA/ISAS, Via Beirut 2-4, 34151, Trieste, Italy, nardini@sissa.it

[†]INAF – Osservatorio Astronomico di Brera, Via Bianchi 46 I-23806 Merate, Italy

**SISSA/ISAS, Via Beirut 2-4, 34151, Trieste, Italy

Abstract. Four years after the launch the *Swift* satellite the nature of the Gamma Ray Bursts (GRBs) broadband afterglow behaviour is still an open issue. The standard external shock fireball model cannot easily explain the combined temporal and spectral properties of Optical to X-ray afterglows. We analysed the rest frame de-absorbed and K-corrected Optical and X-ray light curves of a sample of 33 GRBs with known redshift and optical extinction at the host frame. We modelled their broadband behaviour as the sum of the standard forward shock emission due to the interaction of a fireball with the circum-burst medium and an additional component. This description provides a good agreement with the observed light curves despite their complexity and diversity and can also account for the lack of achromatic late times jet breaks and the presence of chromatic breaks in several GRBs lightcurves. In order to test the predictions of such modelling we analysed the X-ray time resolved spectra searching for possible spectral breaks within the observed XRT energy band, finding 7 GRBs showing such a break. The Optical to X-Ray SED evolution of these GRBs are consistent with what expected by our interpretation.

Keywords: gamma-ray sources

PACS: 98.70.Rz

INTRODUCTION

The launch of the *Swift* satellite ([3]) in November 2004 marked a crucial improvement in the knowledge of the properties of the X-ray and optical afterglows of GRBs. *Swift* is able to quickly slew in the direction of the gamma-ray source and thus allowed, through its X-ray telescope XRT (0.3-10 keV), X-ray observations at less than 100s after the trigger for the first time with a precise (few arc sec) localisation of the X-ray source. The on-board Ultra Violet Optical Telescope (UVOT) provides prompt optical observations. With this aid, a large network of ground based robotic telescopes such as ROTSE-III ([1]), TAROT ([7]), RAPTOR ([14]), and REM ([15]), can automatically point the GRB direction without direct human intervention. These facilities opened a new window on the prompt optical and X-ray properties of GRBs soon after the end of the prompt emission phase.

One fundamental finding obtained in the *Swift* –era is that the X-ray light curves at early times are highly complex. A large fraction of GRBs are characterised by an initial typical steep decay of the X-ray flux, followed by a much shallower one lasting up to $10^3 - 10^4$ s. At the end of this “flat” phase, a break in the X-ray light curve occurs (at a time referred to as T_A , [16]) and afterwards the typical steeper power-law decay sets in.

Both the early time steep and the following shallower phases had not been observed before and cannot be easily accounted for within the standard afterglow emission model. Several interpretations of this complexity, and in particular, of the existence of a shallow decay phase have

been put forward (see e.g. [17] for an exhaustive review on the proposed models).

In [4] we proposed a model (so called “late prompt” scenario) to explain the flat phase and the cause of its ending time at T_A . In this scenario, after the standard prompt emission, a prolonged activity of the central engine (as proposed also for late time flares, e.g. [8]) leads to the formation of “shells” with decreasing power and bulk Lorentz factor Γ . The decreasing Γ would allow to see an increased portion of the emitting area, leading to the observed shallow flux decay phase. The characteristic time T_A would correspond to the time when $1/\Gamma$ becomes equal to the jet opening angle θ_j .

The observed (X-ray and optical) radiation during the shallow phase would be thus result as the superposition of a “standard” forward shock afterglow and of the “late prompt” components.

The XRT follow up of GRB afterglows, together with the well sampled multi-wavelength optical photometry, have shown that often the optical light curve does not track the X-ray one and that chromatic breaks in either the X-ray or Optical light curves occur. These can be hardly accounted for in the simplest standard fireball scenario.

Particularly intriguing is the lack of late times achromatic optical and X-rays breaks in the well sampled light curves of some GRBs. In the standard external shock afterglow scenario an achromatic break is expected if the GRB emission is collimated into a jet. If the emitting source is moving towards the observer with a bulk Lorentz factor Γ , when Γ decreases below $1/\theta_j$, the ob-

served light curve is expected to show a break, as the geometric jet collimation “overcome” the relativistic beaming effect. In this framework the jet break time allows an estimate of θ_j ([12, 2]). The geometrical origin of such a break implies its achromaticity: the lack of clear achromatic jet breaks detections in light curves thus casts some doubts either on the GRB geometry or on the standard afterglow emission scenario.

BROAD BAND LIGHT CURVES MODELLING

In [5] we selected a sample of 33 *Swift* long GRBs with known redshift, published estimate of the host galaxy dust absorption, well sampled XRT and optical follow up. We analysed the rest frame optical and X–ray light curves corrected for the effect of Galactic and host galaxy dust and N_H absorption and modelled the multi–wavelength light curves as due to the sum of two separate components excluding the early time steep decay and the flaring activity. The first component is represented by the “standard” forward shock afterglow emission, following the analytical description given in [11]. The second one is treated in a completely phenomenological way with the aim of minimising the number of free parameters and its SED is modelled as a smoothly joining double power–law, namely:

$$L_{2nd}(\nu, t) = L_0(t) \nu^{-\beta_x}; \quad \nu > \nu_b$$

$$L_{2nd}(\nu, t) = L_0(t) \nu_b^{\beta_0 - \beta_x} \nu^{-\beta_0}; \quad \nu \leq \nu_b,$$

where L_0 is a normalisation constant. While this spectral shape is, for simplicity, assumed not to evolve in time, the temporal behaviour of the second component is also described by a double power–law, with a break at T_A and decay indices α_{flat} and α_{steep} (before and after T_A , respectively).

All the optical and X–ray light curves of the GRBs in the sample can be described rather well by our modelling. In 2 cases both the optical and X–ray light curves are dominated by the second, “late prompt”, component; in 4 cases they are both accounted for by the standard afterglow; more frequently the second component dominates in the X–ray band (15 GRBs) while in the optical it does only in 3 GRBs. The standard afterglow component, instead, prevails more often in the optical (19 GRBs) than in the X–ray band (6 GRBs). The remaining light curves can be well described by the two components providing a comparable contribution or dominating the light curves at different times.

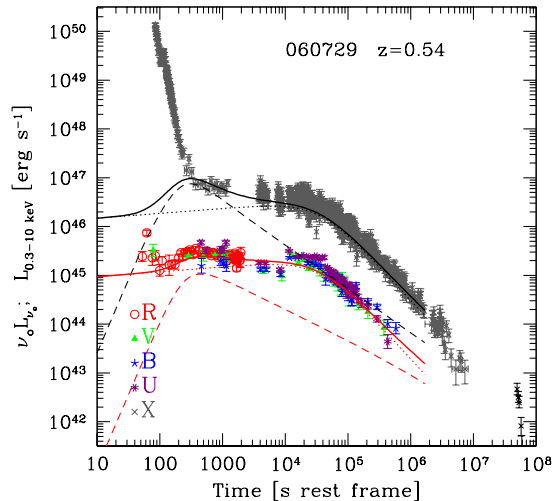


FIGURE 1. X-ray (grey) and optical (different symbols, as labelled) light curves of GRB 060729. Lines represent the model fitting: afterglow (dashed line), late prompt (dotted line) and their sum (solid line). Black lines refer to the X-rays, light grey (red in the electronic version) to the optical. In this GRB, both the optical and the X–rays are dominated by the second component. There is no evidence for an achromatic jet break.

JET BREAKS IN THE TWO COMPONENTS MODELLING

In the proposed scenario, the second component originates from a mechanism different from the standard afterglow emission and no jet break is therefore expected when this dominates the afterglow light curve. If –as proposed – this component arises as postulated in the “late prompt” scenario, no break is expected after T_A . In such a case no information about the jet collimation angle can be inferred from the temporal evolution of the light curve. A “real” jet break would be visible only when the “standard afterglow” emission dominates the late time light curve.

In the two components modelling of the optical and X–ray light curves we can identify different cases in relation to the observation of jet breaks:

- No jet break: if both the optical and X-ray emission are dominated by the second component no break is visible after the end of the “flat” phase e.g. GRB 060729, Fig. 1.
- Achromatic jet break: if both the optical and X-ray emission are dominated by the “standard afterglow” emission, the presence of an achromatic jet break is expected and it is possible to estimate the jet

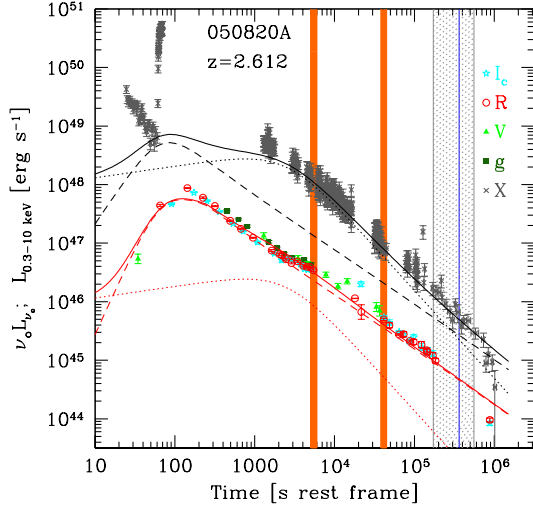


FIGURE 2. X-ray and optical light curves of GRB 050820a. Lines and symbols as in Fig. 1. Grey lines and stripes correspond to the jet break times as reported in the literature (references can be found in [6]). Both the optical and the X-rays are dominated by the “standard afterglow”. There is clear evidence of a break in the optical and a hint of a shallower achromatic break in the X-rays.

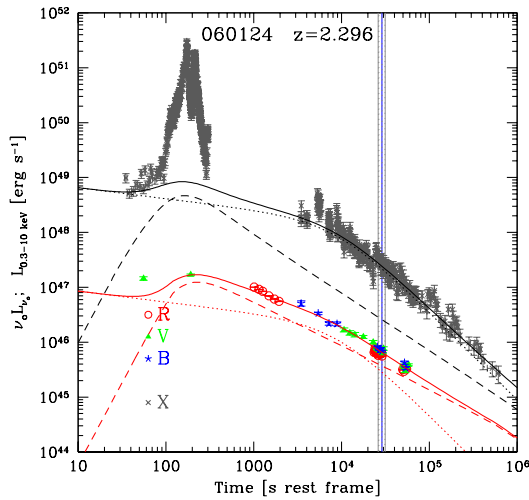


FIGURE 3. X-ray and optical light curves of GRB 060124. Notation as in Fig. 1. Grey lines and stripes correspond to jet break times as reported in the literature (see [6]).

opening angle from the jet break time t_{jet} measure (e.g. GRB 050820a, Fig. 2. As the “standard after-

glow” contributes up to late time in the optical, a jet break is observed. In the X-ray band the second component, instead, prevails only at early times, so when the “standard afterglow” becomes dominant the possible presence of an achromatic break is unveiled.

- Chromatic jet break: sometimes the optical and X-ray light curves are due to different components. Usually the “standard afterglow” and the second component dominate the optical and X-rays bands, respectively. Therefore the “real” jet break is observed in the optical but not in the X-ray light curve, which after T_A can be well fitted by a single power-law e.g. GRB 060124, Fig. 3. Note that in the pre-*Swift* era the X-ray light curves were not as densely sampled as the optical ones, and thus most of the pre-*Swift* jet breaks have been observed only in the optical bands.

In those cases where the light curve is dominated by the “standard afterglow” and a “real” jet break is observed, the post break decay index can appear shallower than what expected in the standard afterglow models. This happens when there is a considerable contribution to the total flux due to the second component. As an example see the X-ray light curve of GRB 050820a (Fig. 2).

SPECTRAL CHECKS

If the optical and the X-ray emission are produced by different processes, the spectra must break between these bands as the process which dominates in one band cannot dominate also in the other. Indeed a spectral break (e.g. the cooling break frequency for the synchrotron emission) between the optical and X-ray bands is sometimes expected also in the standard afterglow scenario (see e.g. Figs. 10 and 11 in [9]). For the light curves modelling we assumed for simplicity that the break frequency ν_b of the second component always falls between the optical and the X-ray bands. However, in some cases ν_b could be within the observed XRT energy range, namely 0.3–10keV. If effectively detected, constraints on the break frequency location and on the low energy spectral index can be inferred. Thus bursts with an observed break in the X-ray spectrum constitute the best candidates for checking the consistency between the optical-to-X-ray SEDs and the light curves modelling.

Figure 4 schematically illustrates the above, namely the predicted optical-to-X-ray SED (right panels) in the different light curve modelling cases (left panels) for the bursts where a spectral break is found in the X-ray spectrum. When the optical and X-ray light curves are dominated by the same component (upper and lower panels), the observed optical fluxes must be consistent with the

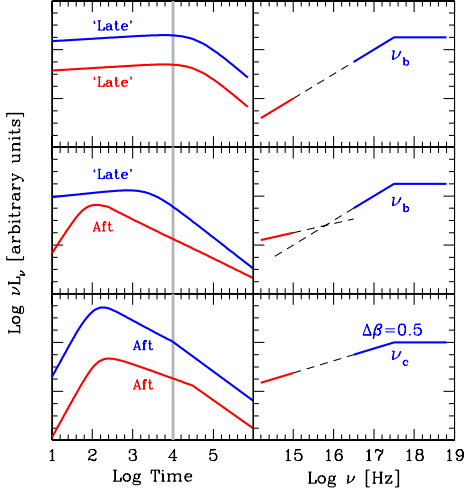


FIGURE 4. Sketch illustrating the possible different cases. The left panels refer to the X-ray (upper) and optical (lower) light curves; the right-hand panels to the corresponding expected optical to X-ray SED. The bottom right panel shows the standard case in which both bands are dominated by the “standard afterglow” component, with a cooling break time appearing first in the X-ray light curve. The vertical grey line indicates the time corresponding to the SED. ν_b is the break frequency of the late component, while ν_c refers to the cooling frequency.

extrapolation of the low energy X-ray spectrum. If they both originate as “standard afterglow” emission (lower panel), the observed break is likely due to the presence of the synchrotron cooling break frequency and the relation between the high energy and the low energy spectral indices (as $\Delta\beta = 0.5$) can be also constrained. When instead the optical and X-ray light curves are dominated by different components (middle panel), the extrapolation of the X-ray spectrum must not significantly contribute to the observed optical fluxes.

X-ray spectral analysis

In order to test for the presence of breaks in the X-ray band, we analysed the XRT spectra of the 33 GRBs of the sample [5], by selecting time intervals not comprising prompt, high latitude emission or flaring activity ([10]). At first the data were fitted with an absorbed single power-law model with frozen Galactic absorption plus a host frame absorption that was left free to vary. We confirm the absence of spectral evolution around T_A , as predicted by the late prompt model that ascribes T_A to

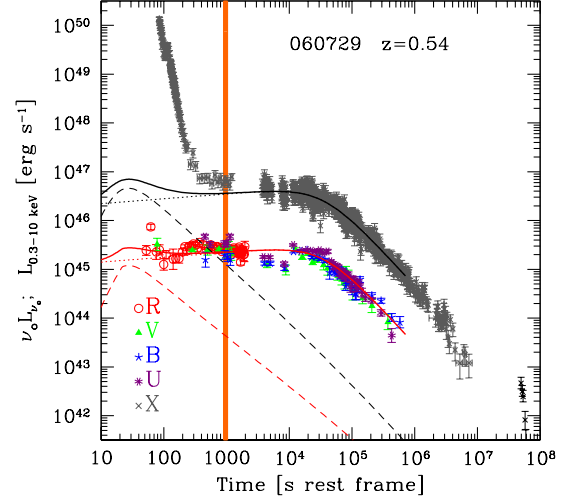


FIGURE 5. X-ray and optical light curves of GRB 060729 in rest frame time. Lines and symbols as in Fig. 1. The vertical solid line indicates the rest frame time of the SED sampling.

a purely geometrical effect. The fitting also confirms the inconsistency between the small A_V^{host} estimated in the optical and the usually large N_H^{host} derived by the X-ray spectral modelling, for a standard N_H/A_V relation (see e.g. Stratta et al. 2004; [13]).

For those spectra with higher photon statistics, a broken power-law model with the same two absorption components was also adopted. In 7 cases the presence of a break in the XRT band provides a fit better than the single power-law case. The broken power-law model is instead excluded (i.e. the break energy falls outside the XRT energy range) in 8 GRBs.

The N_H^{host} derived for the 7 broken power-law fits is smaller than those obtained with a single power-law model, and closer to the values expected from A_V^{host} . However, large N_H^{host} columns are required in some of the GRBs in which a broken power-law fitting is excluded. Thus, while an intrinsic spectral curvature can sometimes account for large N_H/A_V ratios, it cannot be considered a general solution for such a discrepancy.

Optical to X-rays SEDs consistency checks

As discussed above, the 7 GRBs showing a break in the X-ray spectra can provide a consistency check of our two components interpretation. We therefore analysed the optical-to-X-ray SEDs of these events at different times. For each burst, we selected epochs when

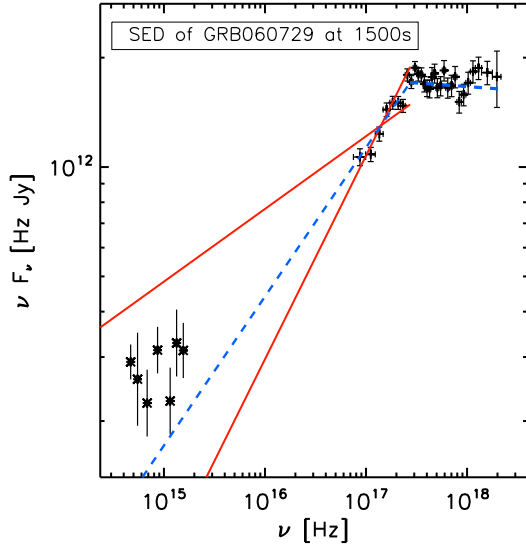


FIGURE 6. Optical to X-ray νF_ν SED of GRB 060729 around 1500 s after trigger in the observer frame (970 s rest frame). The dashed line represents the best fit value of the low energy spectral index $\beta_{X,1}$ and the solid lines correspond to the 90% errors.

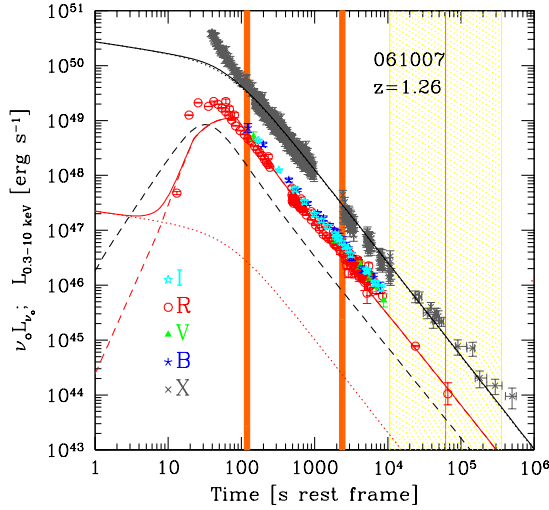


FIGURE 7. X-ray and optical light curves of GRB 061007 in rest frame time. Lines and symbols as in Fig. 1. The vertical solid line indicates the rest frame time of the SED sampling. The vertical stripes refer to the jet break times expected if the burst followed the E_{peak} vs. E_γ Ghirlanda relation ([6]).

simultaneous optical photometry and XRT observations are available, in order to avoid (if possible) flux extrapolations. When the optical and X-ray light curves track each other one single SED is considered, while more SEDs were examined when the two light curves follow different temporal behaviours, to extend the check to various phases of the light curve.

We found that in all the 7 events, the evolution of the broadband SEDs is fully consistent with the predictions of the two components modelling, even in presence of complex light curve behaviours.

As illustrative cases let us consider here two GRBs. Both the optical and X-ray light curves of GRB 060729 are dominated by the second component (see Fig. 5), and thus the optical bands are expected to be consistent with the extrapolation of the low energy X-ray spectral index. The optical-to-X-ray SED shown in Fig. 6 support this prediction. In GRB 061007 the observed optical light curve is dominated by the “standard afterglow” contribution while the second component prevails in the X-ray band. Consistently with our light curve modelling the SEDs (see Fig. 8) show that the low energy extrapolation of the X-ray spectrum does not significantly contribute in the optical bands.

CONCLUSIONS

We considered the optical and X-ray light curves of a sample of well observed long GRBs. We discussed the presence/absence of achromatic jet breaks in the framework of the two components interpretation proposed by [5].

We analysed the X-ray afterglow spectra of the GRBs in order to check for the presence of spectral breaks within the XRT energy range and considered the possible implications of the presence of such a break for the relation between host galaxy dust reddening and N_H column densities. Finally for the 7 bursts with evidence of an X-ray spectral break, we examined the evolution of the optical-to-X-ray SEDs, finding that they are fully consistent with the predictions of the two components light curves modelling.

ACKNOWLEDGMENTS

We acknowledge the Scientific Office of the Embassy of Italy in Egypt for financial support within the framework of the Italian–Egyptian Year of Science and Technology. MN and AC also thank MIUR for partial support. We would also like to thank Fabrizio Tavecchio for useful discussions.

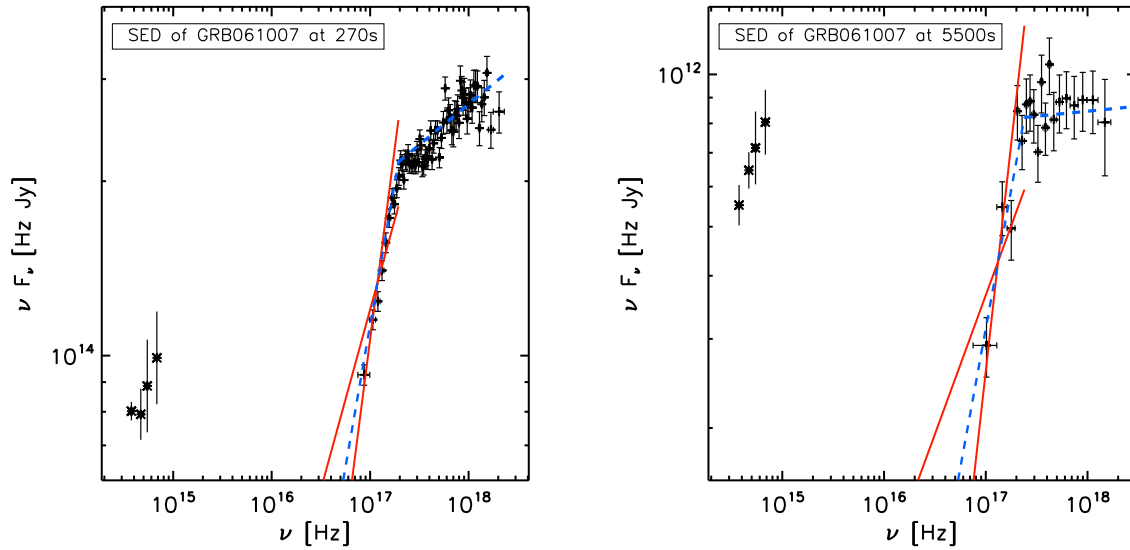


FIGURE 8. Optical to X-ray νF_ν SEDs of GRB 061007 extracted around 270 s (top) and 5500 s (bottom) after trigger in the observer frame (corresponding to 120 s and 2.4 ks in the rest frame). The dashed line represents the best fit value of the low energy spectral index $\beta_{X,1}$ and the solid lines correspond to the 90% errors.

REFERENCES

1. Akerlof, C. W. et al. 2003, *PASP*, **115**, 132
2. Chevalier R.A., & Li Z.Y., *ApJ*, 2000, **536**, 195
3. Gehrels N. et al., 2004, *ApJ*, **601**, 1005
4. Ghisellini G., et al., 2007, *ApJ*, **658**, 75
5. Ghisellini G., et al., 2009, *MNRAS*, **393**, 253
6. Ghirlanda G., et al., 2007, *A&A*, **466**, 127
7. Klotz, A., et al., 2009, *A.J.*, **137**, 4100
8. Lazzati D., Perna R., & Begelman M. C., 2008, *MNRAS*, **388**, L15
9. Nardini M., et al., 2006, *A&A*, **451**, 821
10. Nardini M., et al., 2009, *MNRAS* submitted, preprint(arXiv:0907.4157v1)
11. Panaitescu A & Kumar P., 2000, *ApJ*, **543**, 66
12. Rhoads J.E., 1997, *ApJ*, **487**, L1
13. Schady P., et al., 2007, *MNRAS*, **377**, 284
14. Vestrand W. T., et al., 2004, *Astronomische Nachrichten*, **325**, 549
15. Zerbi R. M., et al. 2001, *Astronomische Nachrichten*, **322**, 275
16. Willingale R. et al., 2007, *ApJ*, **662**, 1093
17. Zhang B., 2007, *Adv. Space Res.*, **40**, 1186